Annealing samples of the superconducting compound Nb_3Au with thermally induced disorder

1992 J. Phys.: Condens. Matter 4 7441

(http://iopscience.iop.org/0953-8984/4/36/017)

J. Phys.: Condens. Matter 4 (1992) 7441–7450. Printed in the UK

Annealing samples of the superconducting compound Nb_3Au with thermally induced disorder

D M R Lo Cascio, P I Loeff and H Bakker

Van der Waals-Zeeman Laboratorium der Universiteit van Amsterdam, Valckenierstraat 65, NL-1018 XE Amsterdam, The Netherlands

Received 18 May 1992

Abstract. To investigate the kinetics of recovery of anti-site disorder in the A15 compound Nb_3Au, isochronal and isothermal annealing procedures at intermediate temperatures (between 833 and 1043 K) were performed on grains quenched from 1355(1) K. From these experiments, the vacancy migration enthalpy and its pre-exponential factor were determined as 0.39 eV and 2.7×10^2 s, respectively. The atomic-migration enthalpy and its pre-exponential factor were found to be 1.43 eV and 7.1×10^{-2} s, respectively. These values will be compared with data for the A15 compound V_3Ga, and for $Ca_3Rh_4Sn_{13}$ which is a superconductor with an A15 substructure, and with data on ball-milled Nb_3Au.

1. Introduction

Nb_3Au is a superconducting compound with an A15 structure. The Au atoms are situated on the corners and in the centre of the unit cell, and the Nb atoms form linear chains. In a previous paper [1] the strong dependence of the superconducting transition temperature, T_c, on the degree of atomic order has been described for Nb_3Au. We assumed that the atomic disorder consists mainly of anti-site defects, i.e. Nb atoms are substituted from the chains on the Au sublattice and Au atoms on the Nb sublattice. The degradation of T_c, due to quenching from high temperatures, was demonstrated to be caused by the atomic disorder that exists at high temperature and which is frozen in by rapid quenching to room temperature. The degree of atomic disorder increases with increasing quenching temperature, which will result in a lower superconducting transition temperature. An Arrhenius type of relation between the superconducting transition temperature and the quenching temperature was derived [1–3]. From this relation the values for the disordering energy of 1.72(6) eV was obtained for the anti-site disorder [1].

In this article the kinetics of the anti-site defects in Nb_3Au during annealing at intermediate temperature are investigated. The analyses of the isotherms are performed with the aid of the equation derived in [4, 5]. The kinetics of the reordering process in quenched material is compared to that in ball-milled material.

2. Theory

The derivation of the equation to analyse the isothermal annealing experiments by [4, 5] was based on the assumption that only the anti-site defects have influence on T_c

0953-8984/92/367441+10$04.50

and that jumping from one sublattice to the other takes place by the usual 'vacancy mechanism'. The dependence of T_c on the vacancy concentration has been neglected since the concentration of vacancies is approximately two magnitudes smaller than the concentration of anti-site defects.

During the quench the equilibrium concentration of anti-site defects at the quenching temperature as well as the equilibrium concentration of thermal vacancies at the quenching temperature are frozen in. Subsequently the samples are annealed. The quenched-in concentrations are higher than the equilibrium concentrations at the lower annealing temperature. This leads to two stages in the recovery process. In the first stage, during which the excess of thermal vacancies are annealed out, the restoration is very fast due to the relatively large amount of vacancies, which enhances the atomic jump rate. The second stage, where there is only an excess of anti-site defects, starts when the excess of vacancies has disappeared. The annihilation rate of the anti-site defects is now equal to the equilibrium rate.

The temperature dependence of the diffusion rate of thermal vacancies will determine the rate at which the excess vacancies will disappear during the anneal at low temperatures. With D_0^v the pre-exponential factor containing the entropy for vacancy migration, h_{1v}^m, the corresponding enthalpy, k the Boltzmann factor and T_a the annealing temperature, the temperature dependence of the diffusivity is given by

$$D^v = D_0^v \exp(-h_{1v}^m/kT_a). \tag{1}$$

The excess of thermal vacancies in the first stage of the anneal will annihilate at grain boundaries and defects. The decrease to zero of these extra thermal vacancies during the anneal will be exponential following

$$\Delta c^v(t) = c^v(t) - c^v(t=\infty) = \Delta c^v(t=0)\exp(-t/\tau^v) \tag{2}$$

with $c^v(t=\infty)$ the equilibrium thermal-vacancy concentration at the annealing temperature, $\Delta c^v(t=0)$ the initial excess of vacancies, t the annealing time and τ^v the relaxation time for the excess vacancy.

The decrease of excess anti-site defects, $\Delta c_B^\alpha = c_B^\alpha(t=\infty) - c_B^\alpha(t)$, due to annealing was assumed to be a first-order process following

$$(d/dt)(\Delta c_B^\alpha) = -\Delta c_B^\alpha/\tau^a(t). \tag{3}$$

Here $\tau^a(t)$ is the characteristic relaxation time of the anti-site defects. This will result in an exponential decrease of the excess anti-site defects. For atomic jumping, vacancies are needed and due to the decreasing vacancy concentration, $\tau^a(t)$ is a function of time by itself. Since the atomic diffusion coefficient is proportional to the vacancy content, τ^a will be proportional to the receiprocal concentration. This leads to

$$\tau^a(t=\infty)/\tau^a(t) = c^v(t)/c^v(t=\infty) \tag{4}$$

with $t^a(t=\infty)$ the equilibrium relaxation time for anti-site defects which will be obtained when the excess of thermal vacancies has been annealed out. Further $c^v(t)$ is the concentration of vacancies after a time t of annealing and $c^v(t=\infty)$ the equilibrium vacancy concentration attained after an infinitely long annealing. After

substituting equation (4) into equation (2) and further equation (2) into equation (3) we get after some algebra the solution of equation (3):

$$\ln\left(\frac{c_B^\alpha(t=\infty)-c_B^\alpha(t)}{c_B^\alpha(t=\infty)-c_B^\alpha(t=0)}\right)=-\frac{t}{\tau^a}+\frac{\tau^v\,\Delta c^v(t=0)}{\tau^a c^v(t=\infty)}\left[\exp\left(\frac{-t}{\tau^v}\right)-1\right]. \tag{5}$$

In [5] the concentration of anti-site defects was taken to be proportional to the degradation of T_c for small concentrations of anti-site defects. This resulted in the equation

$$\ln\left(\frac{c_B^\alpha(t=\infty)-c_B^\alpha(t)}{c_B^\alpha(t=\infty)-c_B^\alpha(t=0)}\right)=\ln\left(\frac{T_c(t=\infty)-T_c(t)}{T_c(t=\infty)-T_c(t=0)}\right) \tag{6}$$

with $T_c(t=\infty)$ the equilibrium transition temperature after annealing for an infinitely long time at the annealing temperature and $T_c(t=0)$ the transition temperature before annealing, thus immediately after quenching.

Fähnle [6] found, on the basis of theoretical and empirical considerations, the relation between the long-range order parameter and the superconducting transition temperature. The relation appeared to be universal for all A15 Nb compounds.

This equation derived by Fähnle was

$$T_c(s)/T_{c\max}=0.17+0.83\exp[-7.78(1-s)] \qquad c_b^\alpha=(1-s)/4 \tag{7}$$

where s is the long-range order parameter, and $T_{c\max}=T_c(s=1)$ the transition temperature for the completely ordered compound. In fact the former assumption (equation (6)) $\Delta T_c \propto (1-s)$ corresponds to the first term of the Taylor expansion of equation (7). We derived with the aid of equation (7) a more general form than equation (6).

From equation (7) we get for the following relation between c_B^α and T_c:

$$c_B^\alpha=\frac{-1}{4\times 7.78}\ln\left(\frac{T_c}{0.83\times T_{c\max}}-\frac{0.17}{0.83}\right). \tag{8}$$

Using this relation we get for the left-hand side of equation (5):

$$\ln\left(\frac{c_B^\alpha(t=\infty)-c_B^\alpha(t)}{c_B^\alpha(t=\infty)-c_B^\alpha(t=0)}\right)=\ln\left[\ln\left(\frac{T_c(t=\infty)-0.17T_{c\max}}{T_c(t)-0.17T_{c\max}}\right)\Big/\ln\left(\frac{T_c(t=\infty)-0.17T_{c\max}}{T_c(t=0)-0.17T_{c\max}}\right)\right]. \tag{9}$$

In figure 1 equation (8) is given as a function of T_c. The approximation used in equation (6) is a fit to a straight line of $\Delta T_c=T_c(t=\infty)-T_c(t=0)$ around $T_c(t=0)+0.5\,\Delta T_c$.

To analyse the experimental results and to fit the data, the right-hand sides of equations (5) and (9) will be used. In figure 2 an isothermal annealing plot is presented. The slope of the tail of the recovery curve gives $1/\tau^a$. The time after which the recovery process passes from stage 1 to stage 2 is τ^v. The intersection of the extrapolation of the tail of the curve with the vertical axis is given by

$$-\tau^a\,\Delta c^v(t=0)/\tau^v c^v(t=\infty). \tag{10}$$

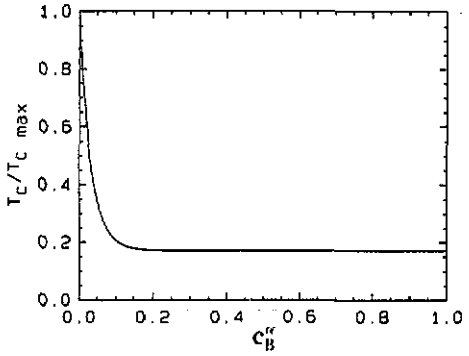

Figure 1. The relation between T_c and c_B^α as described in equation (8).

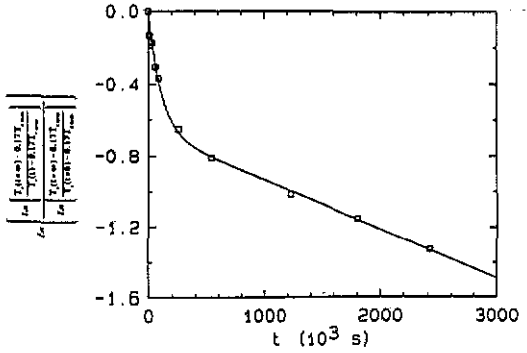

Figure 2. An isothermal annealing plot for Nb_3Au.

From the temperature dependence of τ^a and τ^v we get the activation enthalpies for the anti-site defect annihilation process and the vacancy migration, respectively, together with their pre-exponential factors.

In principle, the formation enthalpy for vacancies can be calculated from the values for $(\tau^a \Delta c^v(t=0))/(\tau^v c^v(t=\infty))$. During the time it takes to bring the sample to the annealing temperature, already some of the excess vacancies are annealed out. The annihilation and migration rates are temperature-dependent quantities and will thus vary during this heating time. The heating time is different for each annealing temperature, which results in different starting points. This has a large influence on the value for the intersection with the vertical axis as a function of annealing temperature. The part of the curve which gives τ^a is almost unaffected by this problem. For τ^v this could implement an extra error.

3. Experimental procedure

The Nb_3Au compound was prepared by arcmelting Nb and Au (both with a purity better than 99.5%) together in the 3 to 1 composition. X-ray diffraction showed a pure A15 diffraction pattern with a lattice parameter of 5.2037(2) Å. After annealing the sample for 20 hours at 1043(1) K, the superconducting transition temperature became 11.39 K. A special quenching device, called HIPOQ [7], was used to quench the sample from high temperature into water. The quenching rate is estimated to be 5×10^4 K s^{-1}. To ensure fast quenching, a powdered sample with powder

diameters between 0.21 mm and 0.48 mm was used. After annealing at 1355(1) K in the HIPOQ, long enough to obtain thermodynamic equilibrium, the sample was quenched into water. The onset T_c of the samples after quenching is 9.588(5) K.

After the quench isochronal and isothermal anneals were performed, all on grains from one single batch quenched from 1355(1) K. To prevent compositional variations and a difference in heat treatment between various grains, the grains were all quenched together. After quenching, the powder was divided into several portions, wrapped in tantalum foil and encapsulated in quartz tubes, which were evacuated and subsequently filled with 0.1 atm pure argon before sealing. The annealing took place in Tempress diffusion furnaces, in which the temperature could be controlled to within 1 K and kept constant to within 0.1 K over a distance of about 50 cm.

The superconducting transition temperature was determined by AC susceptibility measurements. The superconducting transition temperature T_c was taken as the temperature where the susceptibility becomes 'zero', the so-called onset T_c. It was checked for different measuring fields that there was negligible dependence of T_c on the value of the small measuring field.

4. Experimental results

In figure 3 we present the AC susceptibility versus temperature for the Nb_3Au quenched from 1355 K (curve a) for the material annealed at 966 K, after quenching for 3 days (curve b) and annealed for 21 days at the same temperature (curve c).

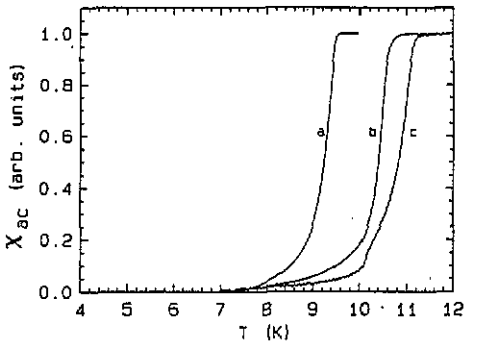

Figure 3. AC susceptibility curves for (*a*) quenched Nb_3Au, (*b*) Nb_3Au annealed at 966 K for 3 days and (*c*) annealed for 21 days at 966 K.

From the isochronal plot shown in figure 4 we see that after 20 hours of annealing at 1040 K the recovery of T_c (11.39 K) is almost complete. From previously performed quenching experiments on samples from the same batch, the maximum value for the superconducting transition temperature $T_{c\,max}$ was found to be 11.75(2) K [1].

In figure 5 the isothermal annealing plot is given for the three lower annealing temperatures (874, 903 and 931 K), and in figure 6 the plot for the other three, higher, annealing temperatures (946, 966 and 1006 K). The lines in these plots are the fits of the experimental data to equation (5). From these fits we get the values for the parameters τ^a, τ^v and $(\tau^a \Delta c^v(t=0))/(\tau^v c^v(t=\infty))$ versus the annealing temperature T_a. These values are shown in table 1 for various values of T_a.

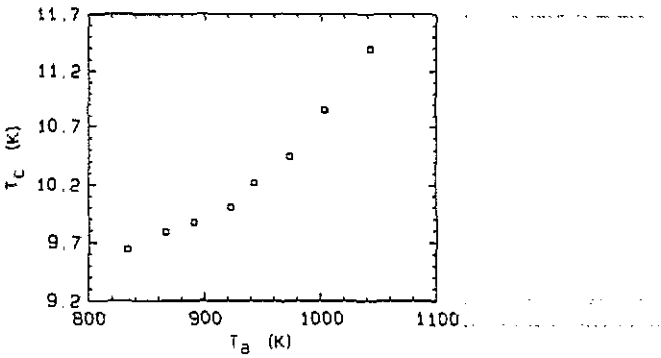

Figure 4. The isochronal annealing plot for Nb_3Au samples quenched from 1355(1) K and annealed for 20 hours at different temperatures.

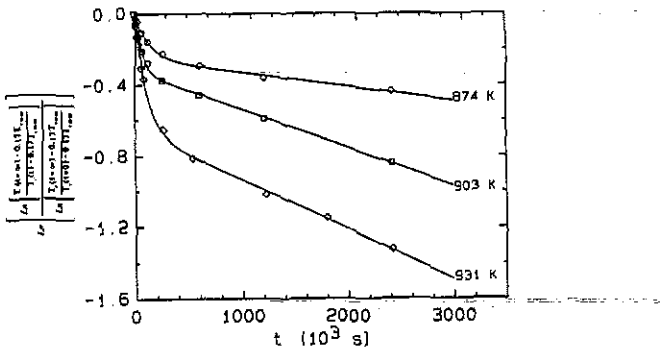

Figure 5. The isothermal annealing plot for Nb_3Au samples quenched from 1355(1) K and annealed at 874, 903 and 931 K.

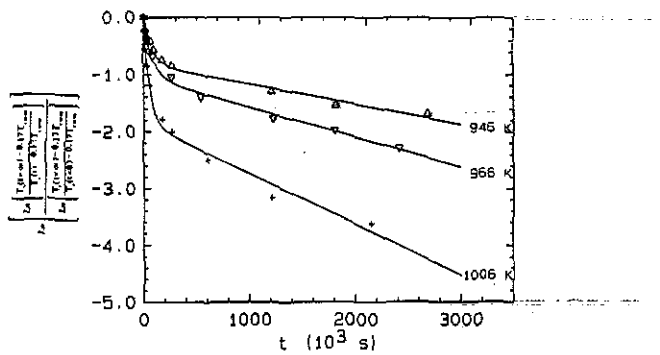

Figure 6. The isothermal annealing plot for Nb_3Au samples quenched from 1355(1) K and annealed at 946, 966 and 1006 K.

The relationship between the relaxation time and temperature is given by equation (1), with D^v the relaxation time and h_{1v}^m the enthalpy belonging to the process. If we plot the logarithm of τ^a or τ^v versus the reciprocal annealing temperature we should get a straight line. The slope of these lines gives the enthalpy for the anti-site defect annihilation and the enthalpy for vacancy migration respectively.

Table 1. The values for τ^a, τ^v and $(\tau^a \Delta c^v(t=0))/(\tau^v c^v(t=\infty))$ versus annealing temperature for Nb_3Au.

T_a (K)	τ^a (s)	τ^v (s)	$\frac{\tau^a \Delta c^v(t=0)}{\tau^v c^v(t=\infty)}$
874	12.22×10^6	12.97×10^4	0.248
903	4.640×10^6	6.478×10^4	0.324
931	3.602×10^6	10.78×10^4	0.659
946	2.878×10^6	8.383×10^4	0.827
966	1.925×10^6	8.266×10^4	1.058
1006	1.114×10^6	5.244×10^4	1.841

The logarithm of the values for τ^a versus the reciprocal annealing temperature is given in figure 7. From the slope, an anti-site annihilation enthalpy h^a of 1.31(6) eV is found. The pre-exponential factor is 0.3(4) s. In figure 7 this fit is represented by the straight line.

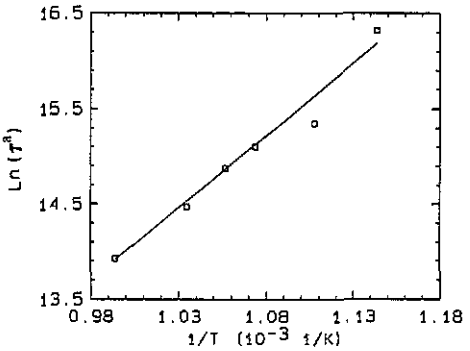

Figure 7. The Arrhenius plot for the logarithm of τ^a versus reciprocal anneal temperature T_a for Nb_3Au. From the slope, h^a is obtained.

Figure 8 gives the Arrhenius curve for τ^v. From this plot we get for the vacancy migration enthalpy h^m_{1v} a value of 0.54(6) eV together with a pre-exponential factor of $1.8(4) \times 10^2$ s. The straight line in figure 8 is again the fit to the measured data. We now will compare the results on Nb_3Au with previous measurements on $Ca_3Rh_4Sn_{13}$ performed by Westerveld *et al* [3] and measurements on the A15 compound V_3Ga performed by Van Winkel *et al* [4]. $Ca_3Rh_4Sn_{13}$ is a ternary superconductor with an A15 substructure. To compare the results with the annealing measurements on V_3Ga, the results on V_3Ga must be reanalysed.

Van Winkel *et al* only calculated the anti-site defect annihilation enthalpy h^a from the obtained data. From the data for τ^v (see table 2) as a function of temperature, a vacancy migration energy of 1.42(7) eV can be found together with a pre-exponential factor of $5.0(46) \times 10^{-8}$ s. The Arrhenius plot for τ^v versus T_a is shown in figure 9.

To calculate $(\tau^a \Delta c^v(t=0))/(\tau^v c^v(t=\infty))$ from the data found for V_3Ga we use the equation

$$\tau^v[c^v(t=0) - c^v(t=\infty)]/\tau^a c^v(t=\infty) = [\alpha c^v(t=0) - 1/\tau^a]\tau^v \tag{11}$$

with α given by

$$\alpha = (D_0^v/c^v)\exp(-h^m_{1v}/kT_a) = D^v/c^v \tag{12}$$

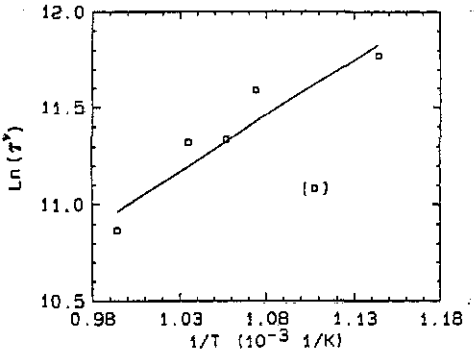

Figure 8. The Arrhenius plot for the logarithm of τ^v versus reciprocal anneal temperature T_a for Nb_3Au. From the slope, h^m_{1v} is obtained.

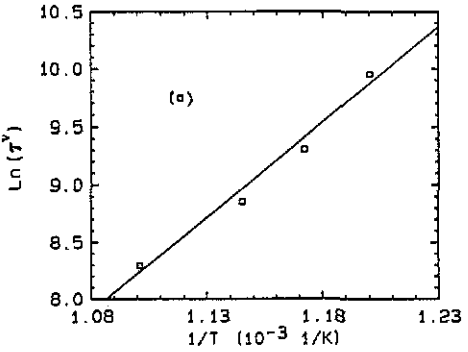

Figure 9. The Arrhenius plot for the logarithm of τ^v versus reciprocal anneal temperature T_a for V_3Ga. From the slope, h^m_{1v} is obtained.

Table 2. The values for τ^a, τ^v, $\alpha c_v(t=0)$ and $(\tau^a \Delta c^v(t=0))/(\tau^v c^v(t=\infty))$ versus annealing temperature for V_3Ga from [4].

T_a (K)	τ^a (s)	τ^v (s)	$1/(\alpha c^v(t=0))$ (s)	$\frac{\tau^a \Delta c^v(t=0)}{\tau^v c^v(t=\infty)}$
833	3.70×10^4	$21(1) \times 10^3$	10.2×10^4	0.15
853	18.5×10^4	$11.0(4) \times 10^3$	3.32×10^4	0.28
873	10.8×10^4	7×10^3	1.50×10^4	0.40
894	6.67×10^4	$17(2) \times 10^3$	1.74×10^4	0.75
908	3.04×10^4	4×10^3	5.34×10^3	0.62

with D^v the temperature dependence of the vacancy diffusivity as given by equation (1). The values for $1/(\alpha c^v(t=0))$ found by Van Winkel [4] are shown in column 4 of table 2. In column 5 of table 2 the values for $(\tau^a \Delta c^v(t=0))/(\tau^v c^v(t=\infty))$, calculated with the aid of equation (11) using data from [4] are shown.

In table 3 the values for the disordering enthalpy and the ordering activation enthalpy are given for Nb_3Au, V_3Ga and $Ca_3Rh_4Sn_{13}$. The values of $2W$ were discussed in a previous article [3]. The value of h^a turns out to be lower for Nb_3Au than for the other compounds. This is a somewhat unexpected result, because diffusion activation enthalpies usually scale roughly with melting temperatures. There is, however, a difference between Nb_3Au and V_3Ga. The components of Nb_3Au are both

transition metals, whereas V_3Ga consists of a transition metal and a non-transition metal. The atomic size difference between Nb and Au is also considerably smaller than between V and Ga. But what the consequences of these facts are on the kinetics in these compounds is not *a priori* clear.

Table 3. The values for the anti-site defect creation enthalpy ($2W$), anti-site defect annihilation enthalpy (h^a), pre-exponential factor (τ_0^a), vacancy migration enthalpy (h_{1v}^m) and pre-exponential factor (D_0^v) for three different compounds.

	Nb_3Au	V_3Ga	$Ca_3Rh_4Sn_{13}$
$2W$ (eV)	1.72(8)	1.23(6)	1.17(4)
h^a (eV)	1.31(6)	2.15(7)	2.14(10)
τ_0^a (s)	$3.0(40) \times 10^{-1}$	$3.6(33) \times 10^{-8}$	$9.3(17) \times 10^{-10}$
h_{1v}^m (eV)	0.50	1.42	0.89
D_0^v (s)	1.8×10^{2}	5.0×10^{-5}	1.3×10^{-3}

From the scatter of the measuring points in figures 8 and 9 it is clear that not too much meaning can be attached to the values of h_{1v}^m obtained. The value of h_{1v}^m seems to be lower for Nb_3Au than for V_3Ga.

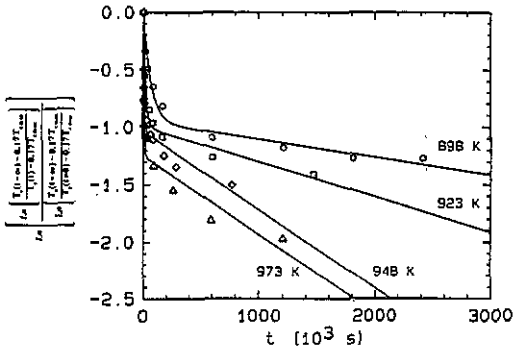

Figure 10. The isothermal annealing plot for ball-milled Nb_3Au samples annealed at 898, 923, 948 and 973 K. Data by Loeff [8].

Table 4. The values for τ^a versus annealing temperature for annealing of ball-milled Nb_3Au obtained from data by Loeff [8].

T_a (K)	τ^a (s)
898	6.44×10^{6}
923	3.26×10^{6}
948	1.45×10^{6}
973	1.45×10^{6}

An important motivation for the present investigation was a comparison of the re-ordering kinetics of quenched and ball-milled materials. We know now that both

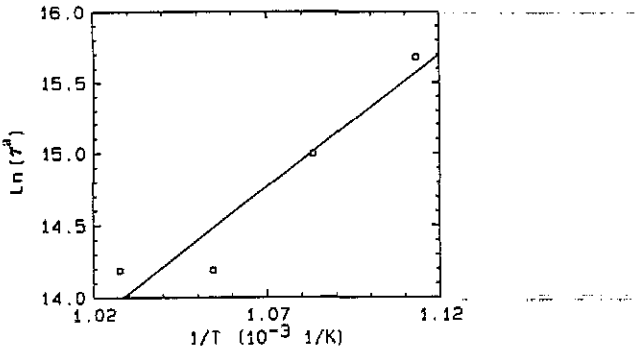

Figure 11. The Arrhenius plot for the logarithm of τ^a versus reciprocal anneal temperature T_a for Nb_3Au, obtained from data by Loeff [8].

techniques lead to atomic disordering of the compound. However, the T_c degradation due to ball-milling is more severe than after quenching. Loeff [8] used a measurement of the decrease of the superconducting transition temperature due to anti-site disorder to monitor the disordering process induced by mechanical attrition. After ball-milling Nb_3Au for approximately 12 hours, the superconducting transition temperature decreased to values of 5.5 or 5.6 K for two different batches. Also the recovery of these samples was studied by Leoff [8] at four different annealing temperatures: 898, 923, 948 and 973 K. Since the amount of disorder introduced by ball-milling is large, for an analysis we had to use equation (9). Using this equation it was possible to make reasonable fits to the data of Loeff [8] (see figure 10). Again, we do not attach too much meaning to the results obtained from the first part of the curves. The τ^a values (table 4), obtained from the second part of the curves, are plotted in figure 11 as a function of reciprocal temperature. Although the number of measuring points is small and the scatter is considerable, we made a straight-line fit as given in figure 11. In this way we obtained a value for the activation enthalpy for the reordering process of 1.61 eV, which is in reasonable agreement with the value of 1.31 eV, measured on quenched samples. This indicates once more that for longer times, when the first annealing process is complete, we have to deal with the same process of reordering by an equilibrium concentration of vacancies.

References

[1] Lo Cascio D M R and Bakker H 1991 *J. Phys.: Condens. Matter* 3 5227
[2] Westerveld J P A and Bakker H 1986 *Phil. Mag.* B 54 L15
[3] Westerveld J P A, Lo Cascio D M R and Bakker H 1987 *J. Phys. F: Met. Phys.* 17 1963
[4] van Winkel A and Bakker H 1985 *J. Phys. F: Met. Phys.* 15 1565
[5] Westerveld J P A, Lo Cascio D M R, Bakker H, Loopstra B O and Goubitz K 1989 *J. Phys.: Condens. Matter* 1 5689
[6] Fähnle M 1982 *J. Low Temp. Phys.* 46 3
[7] Riemersma A J, Manuputy R J D, Schlatter H, Moolhuyzen W F, Rik R, Lo Cascio D M R and Loeff P I 1991 *Rev. Sci. Instrum.* 62 1084
[8] Loeff P I 1990 *Thesis* University of Amsterdam p 81